

Studies of Copper Complexes Displaying N₃S Coordination as Models for Cu_B Center of Dopamine β -Hydroxylase and Peptidylglycine α -Hydroxylating Monooxygenase

Frédéric Champloy, Nourredine Benali-Chérif, Pascale Bruno, Ingrid Blain, Marcel Pierrot, and Marius Réglér*

Chimie, Biologie et Radicaux Libres, UMR CNRS 6517, Universités d'Aix-Marseille 1 et 3, Faculté des Sciences et Techniques de Saint Jérôme, case 432, avenue Escadrille Normandie-Niemen, 13397 Marseille Cedex 20, France

Alain Michalowicz

Laboratoire pour l'Utilisation du Rayonnement Electromagnétique, Bâtiment 209D, Centre Universitaire de Paris-Sud, 91405 Orsay Cedex, France

Received July 24, 1997

We describe the studies of new copper complexes [MeSPY2]CuPF₆, **2**, and [MeSPY2]Cu(ClO₄)₂·CH₃CN, **3**, as models for the Cu_B center of dopamine β -hydroxylase and peptidylglycine α -hydroxylating monooxygenase. The structure of [MeSPY2]Cu(ClO₄)₂·CH₃CN, **3**, has been established by X-ray crystallography. The copper coordination exhibits a square pyramidal geometry where the equatorial plane is occupied by the SCH₃ group and three nitrogen atoms (tertiary amine, one pyridine, and acetonitrile solvent), whereas the axial position binds the second pyridine. Using FEFF calculations and multiscattering interaction, EXAFS refinements show that the SMe group lies in the coordination sphere of copper complexes [MeSPY2]CuPF₆, **2**, and [MeSPY2]Cu(ClO₄)₂·CH₃CN, **3**. While [MeSPY2]CuPF₆, **2**, reacts with dioxygen in dichloromethane without oxidation of the ligand, we observed an oxidation of the sulfide ligand when [MeSPY2]Cu(ClO₄)₂·CH₃CN, **3**, reacts with hydrogen peroxide in methanol. Considering results, we propose that Met³¹⁴, crucial for DBH and PHM activity, could be the site of the H₂O₂ (or ascorbate) inactivation by oxidation to the sulfoxide group.

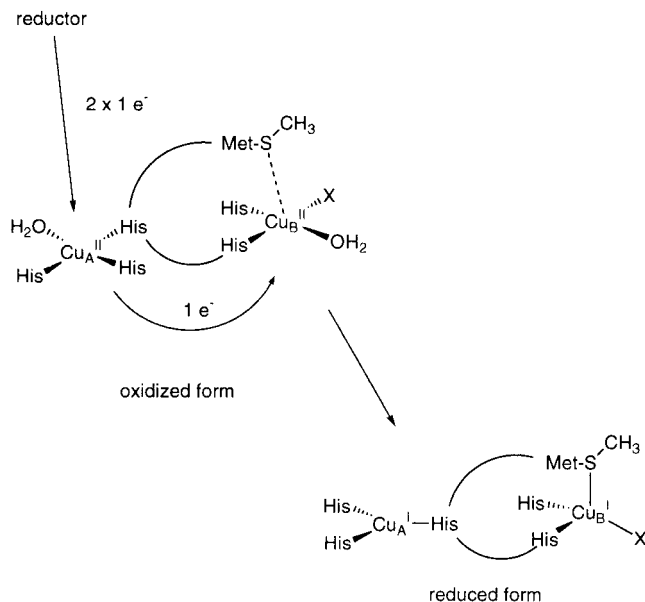
Introduction

Dopamine β -hydroxylase (DBH; EC 1.14.17.1),^{1,2} a copper-containing monooxygenase present in a variety of mammalian tissues, catalyzes the benzylic hydroxylation of dopamine into norepinephrine. All known results from EPR,³ ESEEM,⁴ EXAFS,⁵ and biochemical studies⁶ suggest that DBH contains two inequivalent copper atoms per active site. A Cu_A site is proposed to be the ascorbate binding site, where this reductor delivers one electron at a time. At a distance greater than 4 Å, a Cu_B center involved in dioxygen fixation is responsible for the hydroxylation of dopamine.⁷ Whereas it is well established

that oxidized DBH has a Cu_A(His)₃(H₂O)···Cu_B(His)₂X(H₂O) type of configuration, the structure of the reduced form is not really clear. EXAFS data of reduced DBH show the loss of two water molecules with the appearance of one-half of a sulfur ligand per copper(I) center. While this S ligand, assigned to a Met residue, was first proposed to be coordinated to the Cu_A center,⁴ a recent preparation of one-half apo reduced DBH form seems to demonstrate that the MetS ligand was coordinated to the Cu_B center.⁸ This MetS ligand which is not detected by EXAFS in the oxidized DBH form could be also present but as a weakly bound axial ligand. In addition, DBH presents some structural and functional similarities with another copper-containing monooxygenase, peptidylglycine α -hydroxylating monooxygenase (EC 1.14.17.3, PHM) which catalyses the α -amidation of several bioactive peptides.^{2,9,10} The amino acid sequences of rat PHM and rat DBH exhibit 32% identity over a 291-amino acid region, and some residues in PHM are conserved in DBH. Mutation of the Met residues common to PHM and DBH to Ile have identified Met³¹⁴ as being crucial for catalytic activity. Therefore, we decided to focus our

- (1) Villafranca, J. J. *Metal Ions in Biology*; Spiro, T. G., Ed.; John Wiley and Sons: New York, 1981; Vol 3, pp 263–290. Stewart, L. C.; Klinman, J. P. *Annu. Rev. Biochem.* **1988**, *57*, 551.
- (2) Klinman, J. P. *Chem. Rev.* **1996**, *96*, 2541.
- (3) Blackburn, N. J.; Collison, D.; Sutton, J.; Mabbs, F. E. *Biochem. J.* **1984**, *220*, 447. Blackburn, N. J.; Concannon, M.; Khosrow Shahiyan, S.; Mabbs, F. E.; Collison, D. *Biochemistry* **1988**, *27*, 6001.
- (4) McCracken, J.; Desai, P. R.; Papadopoulos, N. J.; Villafranca, J. J. *Biochem.* **1988**, *27*, 4133.
- (5) Hasnain, S. S.; Diakun, G. P.; Knowles, P. F.; Binsted, N.; Garner, C. D.; Blackburn, N. J. *Biochem.* **1988**, *221*, 545. Scott, R. A.; Sullivan, R. J.; De Wolf, W. E., Jr.; Dolle, R. E.; Kruse, L. I. *Biochemistry* **1988**, *27*, 5411. Blumberg, W. E.; Desai, P. R.; Powers, L.; Freedman, J. H.; Villafranca, J. J. *J. Biol. Chem.* **1989**, *264*, 6029. Pettingill, T. M.; Stange, R. W.; Blackburn, N. J. *J. Biol. Chem.* **1991**, *266*, 16996. Blackburn, N. J.; Hasnain, S. S.; Pettingill, T. M.; Stange, R. W. *J. Biol. Chem.* **1991**, *266*, 23120.
- (6) Stewart, L. C.; Klinman, J. P. *Biochemistry* **1987**, *26*, 5302. Brenner, M. C.; Murray, C. J.; Klinman, J. P. *Biochemistry* **1989**, *28*, 4656.
- (7) Anh, N.; Klinman, J. P. *Biochemistry* **1983**, *22*, 3090. Miller, S. M.; Klinman, J. P. *Biochemistry* **1985**, *24*, 2114.

- (8) Blackburn, N. J. In *Bioinorganic Chemistry of Copper*; Karlin, K. D., Tyeclar, Z., Eds.; Chapman & Hall: New York, 1993; pp 164–183. Reedy, B. J.; Blackburn, N. J. *J. Am. Chem. Soc.* **1994**, *116*, 1924.
- (9) Boswell, J. S.; Reedy, B. J.; Kulathila, R.; Merkler, D.; Blackburn, N. J. *Biochemistry* **1996**, *35*, 12241.
- (10) During the writing of this article, the X-ray structure of the oxidized form of PAM was solved by Prigge, S. T.; Kolhekar, A. S.; Eipper, B. A.; Mains, R. E.; Amzel, L. M. *Science* **1997**, *278*, 1300. This work confirms the presence of a Met residue as a weakly bound ligand in the coordination sphere of the Cu_B center ($d_{\text{Cu-SMet}} = 2.68 \text{ \AA}$).

Scheme 1. Blackburn Model for the Oxidized and Reduced DBH and PHM Active Sites (X Could Be either a His or an O-donor ligand)

attention on the chemistry and the X-ray spectroscopy of copper ions with N₃S-type ligand. We report here the synthesis, the characterization by X-ray spectroscopies, and the reactivity toward dioxygen and hydrogen peroxide of copper complexes coordinated to MeSPY2 ligand **1** (Scheme 1).

Experimental Section

General Methods. Solvents were freshly distilled under nitrogen: MeOH from magnesium, diethyl ether from sodium benzophenone ketyl, and acetonitrile from calcium hydride. Deoxygenation of solvents and solutions was carried out by three vacuum/purge cycles. Commercial starting materials were used without further purification, except for 2-vinylpyridine which was distilled prior to use. Cu(CH₃CN)₄PF₆ was obtained by reaction of Cu₂O with HPF₆ in deoxygenated acetonitrile.¹¹ Preparations and handling of air-sensitive compounds were carried out by using standard Schlenk techniques. ¹H and ¹³C NMR spectra were recorded on a Bruker AC-200 spectrometer. Chemical shifts are reported as δ values in ppm downfield from TMS as internal standard. Elemental analyses were obtained on a CHN Technicon microanalyzer.

N-2-(Methylthio)ethyl-N-bis-2-(2-pyridyl)ethylamine (MeSPY2, 1). Freshly distilled 2-vinylpyridine (35 g, 0.33 mol), 2-methylthioethylamine (3 g, 33 mmol), and acetic acid (10 g, 0.17 mol) in MeOH (100 mL) were refluxed for 2 days. Then, MeOH was evaporated under vacuum, and 100 mL of 15% NaOH solution was added. After the mixture was extracted with CH₂Cl₂ (3 \times 50 mL), the organic layers were dried over Na₂SO₄. Evaporation of CH₂Cl₂ under reduced pressure (18 mmHg) gave a crude product which still contained 2-vinylpyridine, which was eliminated by vacuum distillation (25 $^{\circ}$ C, 0.01 mmHg). Flash chromatography (silica gel, CH₂Cl₂/MeOH 95:5) of crude product afforded 6.5 g (65%) of amine **1**. Anal. Calcd (found) for C₁₇H₂₃N₃S: C, 67.74 (67.80); H, 7.69 (7.74); N, 13.94 (14.01). ¹H NMR (200 MHz, CD₃CN) δ : 8.46 (dt, *J* 4.6, 1 Hz; 2 H), 7.60 (td, *J* 7.5, 1.6 Hz; 2 H), 7.23–7.03 (m; 4H), 2.89 (bs; 8 H), 2.74 (m; 2 H); 2.47 (m; 2 H); 2.03 (s; 3 H). ¹³C NMR (50 MHz, CD₃CN) δ : 161.46 (2 C), 149.72 (2 CH), 137.10 (2 CH), 124.12 (2 CH), 121.93 (2 CH), 54.34 (2 CH₂), 51.46 (CH₂), 36.72 (CH₂), 35.15 (CH₂), 15.60 (CH₃).

[MeSPY2]CuPF₆, 2. Amine **1** (2 g, 6.6 mmol) and Cu(CH₃CN)₄PF₆ (2.5 g, 6.7 mmol) in deoxygenated acetonitrile (10 mL) were stirred under Ar for 1 h. Copper(I) complex **2** was precipitated by addition of anhydrous diethyl ether. Filtration under Ar and drying under high

Table 1. Experimental Details of the Crystal Structure Determination of Copper(II) Complex 3

formula	C ₁₉ H ₂₆ Cl ₂ CuN ₄ O ₈ S
formula weight	604.95
space group	<i>P</i> 2 ₁ / <i>c</i>
<i>a</i> , Å	14.131(3)
<i>b</i> , Å	14.782(4)
<i>c</i> , Å	12.280(3)
β , deg	97.02(5)
<i>V</i> , Å ³	2545.9(5)
<i>Z</i>	4
<i>d</i> _{calc} , g/cm ³	1.58
μ (Mo K α), cm ⁻¹	11.98
total no. of unique data	4157
no. with $F^2 > 3\sigma(F^2)$	3496
<i>R</i> ^a	0.0568
<i>R</i> _w ^b	0.0657
goodness of fit ^c	1.35
largest shift, esd in final cycle	0.3
largest peak, e/Å ³	+0.78, -0.60

^a $R = \sum ||F_o| - |F_c|| / \sum |F_o|$. ^b $R_w = [\sum_w (|F_o| - |F_c|)^2 / \sum_w |F_o|^2]^{1/2}$; $w = 1/\sigma^2 |F_c|$. ^c $w = (|F_o| - |F_c|)^2 / \sum_w |F_o|^2]^{1/2}$.

vacuum (0.01 mmHg) afforded 2.5 g (73%) of the very air-sensitive yellow copper(I) complex **2**. Anal. Calcd (found) for C₁₇H₂₃N₃S-CuPF₆: C, 40.04 (40.07); H, 4.55 (4.58); N, 8.24 (8.30). ¹H NMR (200 MHz, CD₃CN) δ : 8.56 (bd, *J* 4 Hz; 2 H); 7.80 (bt, *J* 7 Hz; 2 H); 7.50–7.20 (m; 4 H); 2.77 (bs; 12 H); 2.21 (s; 3 H). ¹³C NMR (50 MHz, CD₃CN) δ : 150.99 (2 CH); 138.89 (2 CH); 126.46 (2 CH); 123.81 (2 CH); 54.34 (2 CH₂); 51.46 (CH₂); 36.72 (2 CH₂); 35.15 (CH₂); 18.77 (CH₃).

[MeSPY2]Cu(ClO₄)₂·CH₃CN, 3. Amine **1** (2 g, 6.6 mmol) and Cu(ClO₄)₂·6H₂O (2.5 g, 6.7 mmol) in acetonitrile (10 mL) were stirred for 1 h. Copper(II) complex **3** was precipitated by addition of diethyl ether. Filtration and drying under vacuum (0.01 mmHg) afforded 3.6 g (90%) of blue copper(II) complex **3**. Anal. Calcd (found) for [C₁₇H₂₃N₃S]Cu(ClO₄)₂·CH₃CN: C, 37.72 (37.99); H, 4.33 (4.36); N, 9.26 (9.55).

Crystal Structure Determination. Crystal data for compound **3** with details of the X-ray diffraction experiment are reported in Table 1. Cell constants and the orientation matrix for data collection were obtained from least-squares refinement, using setting angles of 25 reflections in the range 20 $^{\circ}$ < 2 θ < 28 $^{\circ}$. Two intense reflections were recorded throughout the data every hour and showed no decay during the exposure time. The data were corrected for *L*_p but not for absorption and secondary extinction, resulting in the unique set of 3496 reflections with $I > 3\sigma(I)$ used in the structure determination. All non-H atoms were found by direct methods,¹² and the structure was refined successfully in space group *P*2₁/*c* by a full-matrix least-squares procedure using anisotropic thermal parameters for all non-H atoms. The weighting scheme used is

$$w = [\sigma(I_{\text{obs}})^2 + (0.04I_{\text{obs}})^2]^{-1} \quad (1)$$

Full-matrix least-squares refinement based on *F* converged at *R* = 0.0568, *R*_w = 0.0657; *S* = 1.35; (Δ/σ)_{max} = 0.3 for all atoms; residual \pm de = +0.78, -0.60 e Å⁻³ in a final DF synthesis, atomic scattering factors from *International Tables for X-ray Crystallography*.¹³

Positional parameters and selected bond distances and angles with ORTEP perspective view are given in Table 2 and Figure 1, respectively. Perchlorate anions showed high thermal parameters due to disordered positions as indicated in DF maps. Oxygen O4 attached

- (12) Frenz, B. A. The Enraf-Nonius CAD-4 SDP-A Real Time System for Concurrent X-ray Data Collection and Crystal Structure Solution. In *Computing in Crystallography*; Schenk, H., Olthof-Hazekamp, R., Van Koningsveld, H., Bassi, G. C., Eds.; Delft University Press: The Netherlands, 1978.
- (13) *International Tables for X-ray Crystallography*; Ibers, J., Hamilton, W. C., Eds.; Kynoch Press: Birmingham, 1974; Vol. IV. (Present distributor Kluwer Academic Publishers: Dordrecht, The Netherlands.)

(11) Kubas G. J. *Inorg. Synth.* **1979**, *19*, 90.

Table 2. Positional Parameters and Their Estimated Standard Deviation in Copper(II) Complex **3**

atoms	x	y	z	B (Å ²) ^a
Cu	0.78215(4)	0.02430(4)	0.23409(4)	2.93(1)
C1	0.6654(4)	-0.1315(4)	0.2785(5)	5.0(1)
C2	0.6648(5)	-0.0865(4)	0.3887(5)	5.5(1)
C3	0.7269(5)	0.0757(5)	0.4863(5)	6.7(2)
C4	0.6809(4)	-0.1174(4)	0.0859(4)	4.3(1)
C5	0.7841(4)	-0.1362(4)	0.0711(5)	4.6(1)
C6	0.8282(4)	-0.0544(4)	0.0260(4)	3.8(1)
C7	0.8647(4)	-0.0556(5)	-0.0733(5)	5.6(1)
C8	0.8997(5)	0.0243(5)	-0.1120(5)	5.9(1)
C9	0.8971(4)	0.1024(4)	-0.0532(4)	5.1(1)
C10	0.8606(4)	0.0989(4)	0.0459(4)	3.9(1)
C11	0.5812(3)	-0.0118(4)	0.1714(4)	4.2(1)
C12	0.5826(4)	0.0685(4)	0.0928(5)	4.5(1)
C13	0.6200(3)	0.1549(4)	0.1452(4)	3.8(1)
C14	0.5725(4)	0.2361(4)	0.1219(6)	5.6(1)
C15	0.6067(4)	0.3127(4)	0.1725(6)	6.3(2)
C16	0.6876(4)	0.3092(4)	0.2459(6)	5.9(2)
C17	0.7324(4)	0.2277(4)	0.2644(5)	4.9(1)
C18	0.9782(4)	0.1077(4)	0.3232(4)	3.7(1)
C19	1.0756(4)	0.1357(5)	0.3609(5)	5.1(1)
C11	0.6225(1)	-0.1123(1)	0.7061(1)	6.15(4)
Cl2	1.0001(1)	0.32928(9)	0.1470(1)	4.52(3)
N1	0.6718(3)	-0.0633(3)	0.1881(3)	3.39(8)
N2	0.8266(3)	0.0228(3)	0.0847(3)	3.33(8)
N3	0.6997(3)	0.1507(3)	0.2152(3)	3.63(9)
N4	0.9034(3)	0.0855(3)	0.2921(3)	3.77(9)
O1	0.9402(4)	0.2913(4)	0.2155(5)	12.2(2)
O2	1.0725(5)	0.2791(5)	0.1212(6)	16.9(2)
O3	0.9740(6)	0.4075(5)	0.0898(8)	15.0(3)
O4	1.0608(7)	0.3755(7)	0.2274(9)	8.7(3)
O-4	0.9462(9)	0.2994(9)	0.0490(9)	10.6(4)
O5	0.7011(4)	-0.1424(5)	0.6627(5)	10.8(2)
O6	0.6236(5)	-0.1377(6)	0.8130(4)	12.8(2)
O7	0.5970(7)	-0.0311(5)	0.678(1)	28.1(3)
O8	0.5437(5)	-0.1573(8)	0.6560(7)	16.6(3)
S	0.7700(1)	-0.0183(1)	0.4150(1)	4.57(3)

^a Anisotropically refined atoms are given in the form of the isotropic equivalent displacement parameter defined as $\frac{1}{3}[a^2B_{11} + b^2B_{22} + c^2B_{33} + ab(\cos \gamma)B_{12} + ac(\cos \beta)B_{13} + bc(\cos \alpha)B_{23}]$.

to Cl1 was shared into two different positions of equal multiplicity (O4 and O-4).

X-ray Absorption. X-ray absorption measurements were made at LURE-Orsay on XAS II beamline. The storage ring delivered a current of 320 mA at 1.85 GeV. The monochromator was Si(111). The X-ray spectra were recorded in transmission mode using standard He-filled ionization chambers. Energies were calibrated by means of a Cu-foil internal standard, the first inflection point on the Cu edge was assigned as 8978 eV.

EXAFS Data Collection. The spectra were recorded in the transmission mode, the amount of copper complexes in each sample was calculated in order to obtain an edge jump $\Delta\mu(x)$ equal to 1, completed with cellulose powder and compressed as homogeneous pellets (1 mm thick) supported in an Al spacer with 63.5-mm Mylar tape windows. For each sample three XANES (8950 to 9130 eV, 0.35 eV step, 512 points, 2 s/points) and six EXAFS (8900 to 9900 eV, 1.95 eV step, 512 points, 2 s/points) scans were recorded at ambient temperature (295 K). Data reduction was accomplished with the software package "EXAFS pour le Mac".¹⁴ Before being averaged, each spectrum corresponding to one sample is treated separately using standard procedures.¹⁵ Pre-edge background is removed with a linear fit up to the edge and extrapolated using the Lengeler-Eisenberger method.¹⁶ Atomic background μ_0 is removed with a fifth-order

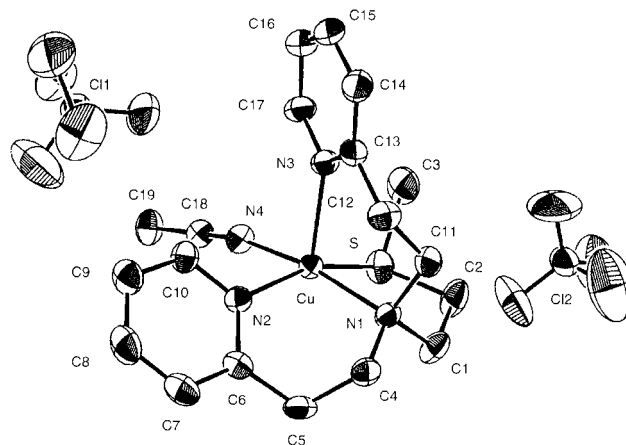


Figure 1. ORTEP perspective view of copper(II) complex **3** displaying the numbering scheme and selected bond distances and angles. Bond distances are in Å: Cu-S, 2.335(1); Cu-N1, 2.052(4); Cu-N2, 2.011(4); Cu-N3, 2.199(4); Cu-N4, 1.990(4). Bond angle are in deg: S-Cu-N, 187.1(1); S-Cu-N2, 158.8(1); S-Cu-N3, 103.3(1); S-Cu-N4, 86.7(1); N1-Cu-N2, 93.1(2); N1-Cu-N3, 97.6(1); N1-Cu-N4, 167.7(2); N2-Cu-N3, 97.7(2); N2-Cu-N4, 88.9(2); N3-Cu-N4, 94.2(2). Numbers in parentheses are the estimated standard deviation in the least significant digits.

polynomial fit in the range 9050–9900 eV, followed with a 6 knots spline fit in the same range. The EXAFS signal is extracted with the standard formula

$$\chi(E) = \frac{[\mu(E) - \mu_0(E)]}{\mu_0(E)} \quad (2)$$

in the range 9006–9900 eV.

The energy origin E_0 was chosen in the edge jump at the maximum of the first-order derivative (8985 eV for **3** and 8990 eV for **2**). These E_0 values will be allowed to vary during the fitting procedure. After extraction of the EXAFS signals on each recording, the average signals $\chi(k)$ and their standard deviations are calculated. These standard deviations are used in the estimation of standard error of the fitted parameters.¹⁷ The systematic errors in the distances between the metal atom and its neighbors are typically estimated as ca. 0.01 and 0.02 Å, respectively, for short and long distances (and 20% for the number of atoms per shell); these values are used in the text. The EXAFS signals were used between 3 and 13 Å⁻¹, and the Fourier transforms of the averaged EXAFS signal $k^3\chi(k)$ multiplied by the Kaiser-Bessel apodization window ($\tau = 2.5$) were calculated in this range. Fourier filtering procedure is used for two purposes (i) to remove the noise (filtering window, 0–13 Å) and (ii) to separate each component of the EXAFS signal when it is possible without spoiling of the data.

Oxidation of [MeSPY2]Cu(ClO₄)₂·CH₃CN, **3, with H₂O₂ in MeOH.** In a Schlenk tube placed under argon and containing 20 mL of deoxygenated MeOH, 100 mg (0.15 mmol) of copper(II) complex **2**, and 150 μ L (1.5 mmol) of 30% H₂O₂ were introduced. After the mixture stood for 2 h at room temperature and after vacuum evaporation of MeOH and dissolution of the residues in 50 mL of CH₂Cl₂, the decomplexation with 35% NH₄OH solution gave 40 mg (84%) of oxidized ligand **4** (MeSOPY₂). ¹H NMR (CDCl₃) δ : 2.40 (s; 3 H), 2.70 (m; 2 H), 2.90 (m; 10 H), 7.05 (m; 4 H), 7.50 (td, *J* 1.7, 7.6 Hz; 2 H), 8.49 (d, *J* 4.6 Hz; 2 H). ¹³C NMR (CDCl₃) δ : 35.85 (2 CH₂), 38.73 (CH₃), 46.92 (CH₂), 53.39 (CH₂), 53.85 (2 CH₂), 121.22 (CH), 123.87 (CH), 136.33 (CH), 149.12 (CH), 160.4 (C).

Results and Discussion

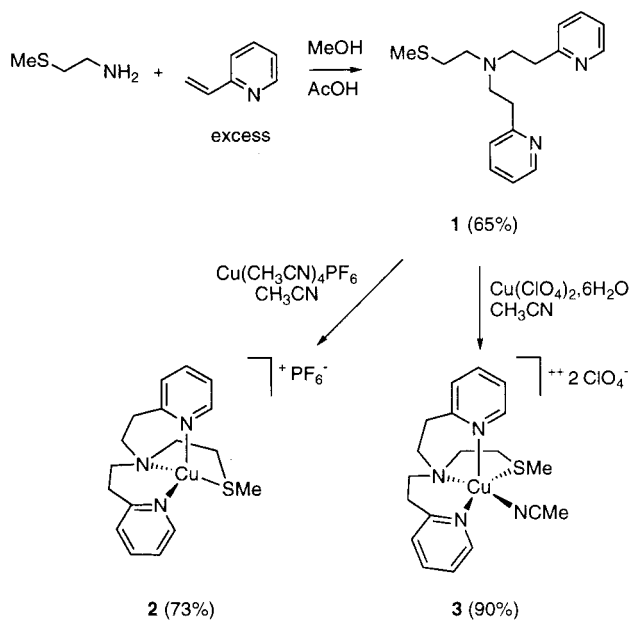
Synthesis. The Michael-type addition of 2-methylthioethylamine to freshly distilled 2-vinylpyridine in a MeOH–acetic

(14) Michalowicz, A. *EXAFS pour le Mac*; Ed. Société Française de chimie: Paris, 1991, p 101.

(15) Teo, B. K. *EXAFS: Basic principles and data analysis*; Springer-Verlag: Berlin, 1986. Koningsberger, D. C., Prins, R., Eds. *X-ray Absorption Principles, Techniques, Applications of EXAFS, XANES, SEXAFS; Chemical Analysis*; Wiley: New York, 1988; Vol. 92.

(16) Lengeler, P.; Eisenberger, X. X. *Phys. Rev.* **1980**, *21*, 4507.

(17) Lytle, F. W.; Stern, E. A.; Sayers D. E. *Physica* **1989**, *B158*, 701. Michalowicz, A. Thèse University of Paris-Val de Marne, 1990.

Scheme 2. Synthesis of Copper(I) and Copper(II) Complexes **2** and **3**

acid mixture leads to ligand **1** in good yields.¹⁸ Interaction of **1** under Ar with 1 equiv of $\text{Cu}(\text{CH}_3\text{CN})_4\text{PF}_6$ in deoxygenated acetonitrile affords the very sensitive pale-yellow copper(I) complex **2** which was isolated by precipitation with anhydrous diethyl ether. Copper(II) complex **3** was obtained in good yields by treatment of 1 equiv of $\text{Cu}(\text{ClO}_4)_2 \cdot 6\text{H}_2\text{O}$ with ligand **1** in acetonitrile. Crystallization of complex **3** (Scheme 2) from a saturated acetonitrile solution using the diethyl ether vapor diffusion technique gave blue crystals which were suitable for X-ray diffraction analysis (Table 1 and Figure 1).

X-ray Structure Description of Copper(II) Complex 3.

The copper coordination exhibits a square pyramidal geometry as is usual for this type of copper complex (Figure 1).¹⁹ The SCH_3 group is perhaps not expected in the axial but in the equatorial position at a distance $\text{Cu}-\text{S}$ of 2.335(2) Å. Three nitrogen atoms complete the equatorial plane, the tripod nitrogen atom N1, the nitrogen pyridine atom N2, and the nitrogen acetonitrile atom N4 with bond distances equal to 2.056(4), 2.011(4), and 1.993(4) Å, respectively. These distances are similar to those found in the literature for the $\text{Cu}-\text{N}$ and the $\text{Cu}-\text{S}$ bonds.²⁰ The pyridine nitrogen atom N3 in the axial position is at 2.209(4) Å, and this type of long $\text{Cu}-\text{N}$ bond has also been observed in other copper complexes.²¹ The central copper atom is out of the plane (N1, N2, N4, S) toward the fifth axial ligand N3, and the distance of the copper to the mean square plane is 0.301(4) Å. The dihedral angle between the two pyridine rings is 99.4(2)°.

EXAFS Studies of Copper Complexes 2 and 3. The XANES spectra at the Cu K edge and their first derivatives are reported in Figure 2. The spectrum of the copper(I) complex **2** is different from that of the copper(II) complex **3**. The first derivative Cu K edge spectra exhibits maxima at 8980 and 8986 eV, respectively, for complexes **2** and **3**, corresponding to the

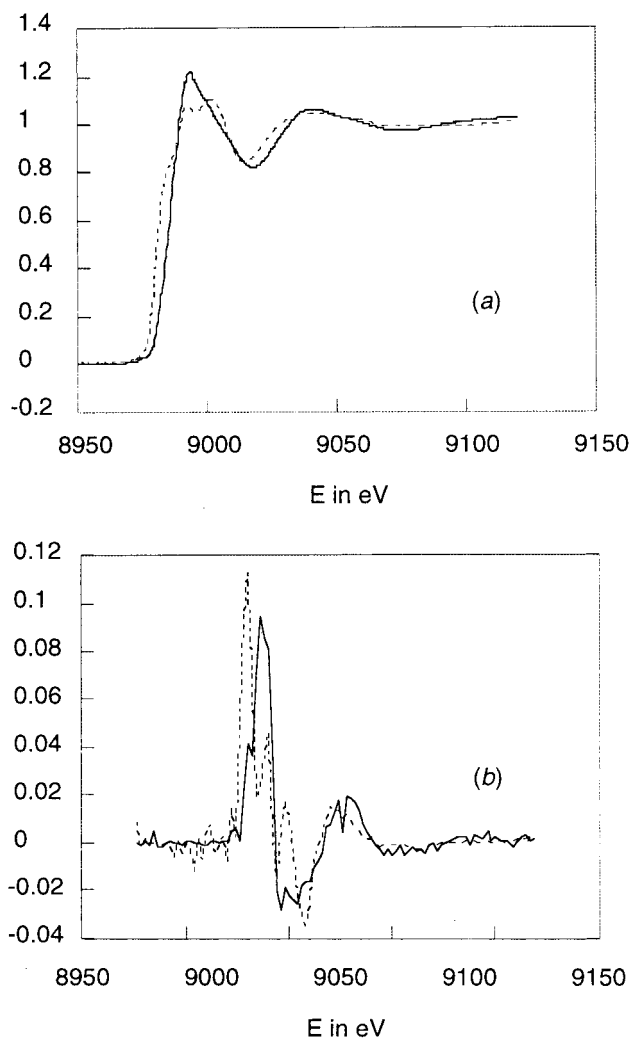


Figure 2. (a) Cu K edge spectra and (b) its first derivative for copper(I) complex **2** (dashed line) and copper(II) complex **3** (solid line).

energy edge. These results are similar to those described in the literature for copper(I) and copper(II) complexes.²²

The analysis of EXAFS spectra was performed by means of FEFF 6.01 code²³ for the ab initio EXAFS calculations using the curved-wave multiple-scattering and X-Fine²⁴ for the optimization of the FEFF input data. The calculations included 201 and 245 unique paths, respectively, for compounds **2** and **3** with effective length <5.1 Å and up to six legs.

Details of the EXAFS refinement are given in Table 3. For both compounds, the varied parameters were the threshold energy E_0 , the scale factor S_0^2 , and the Debye-Waller factors σ^2 for each path. Positional parameters are included in the refinement of compound **2** only. For the EXAFS refinement of **3**, a model comprising the non-H atoms was constructed using the known geometry. Calculations with initial values for S_0^2 (1.0) and $\langle\sigma^2\rangle$ (7×10^{-3}) correspond to an R factor of 37.3% but readily converge with $R = 6.44\%$. However, several steps were necessary for the refinement of compound **2**:

(i) A starting model was constructed on the base of a regular tetrahedral coordination of Cu(I) with three $\text{Cu}-\text{N}$ distances

(18) Karlin K. D.; Hayes J. C.; Gultneh Y.; Cruse R. W.; McKown J. W.; Hutchinson J. P.; Zubieta J. *J. Am. Chem. Soc.* **1984**, *106*, 2121.

(19) Ailou, E. H.; Amadei, E.; Giorgi, M.; Pierrot, M.; Réglie, M. *J. Chem. Soc., Dalton Trans.* **1993**, 549.

(20) Orpen, A. G.; Brammer, L.; Allen, F. H.; Kennard, O.; Watson, D. G.; Taylor, R. *J. Chem. Soc., Dalton Trans.* **1989**, 12, S1. Baker, E. N.; Garrick, P. M. *J. Chem. Soc., Dalton Trans.* **1978**, 416.

(21) Kitajima, N.; Moro-oka, Y. *J. Chem. Soc., Dalton Trans.* **1993**, 2665.

(22) Kau, L. S.; Spira-Solomon, D. J.; Penner-Hahn, J. E.; Hodgson, K. O.; Solomon, E. I. *J. Am. Chem. Soc.* **1987**, *109*, 6433.

(23) Rehr, J. J.; Mustre de Leon, J.; Zabinsky, S. I.; Albers, R. C. *J. Am. Chem. Soc.* **1991**, *113*, 5135.

(24) Champloy, F.; Giorgi, M.; Michalowicz, A.; Pierrot, M. *J. Synchrotron Radiat.* **1997**, *4*, 36.

Table 3. EXAFS Analysis of Copper Complexes 2 and 3

	3		2	
E_0 (eV)	8978.42		8985.78	
S_0^2	1.1029		0.9513	
R factor ^a	3.13(37.3)		7.01(48)	
Fourier transform				
atoms	distances ^b (Å)	σ^2 ($\times 10^{-3}$)	distances ^b (Å)	σ^2 ($\times 10^{-3}$)
N _{pyr}	2.01	5.01	2.00	6.43
N _t	2.06	5.66	1.84	6.76
N _{pyr(axial)}	2.21	29.77	2.00	6.67
S	2.34	6.20	2.16	6.24
N(CH ₃ CN)	1.99	7.08		

^a $R = \sum(k_{\text{exp}}^3(k) - k_{\text{th}}^3(k))^2 / \sum(k_{\text{exp}}^3(k))^2 \times 100$. Refinement starting values in parentheses. ^b Crystallographic values. Filter window 0–12 Å (whole signal). ^c Filter window 0.91–3 Å (first and second shells).

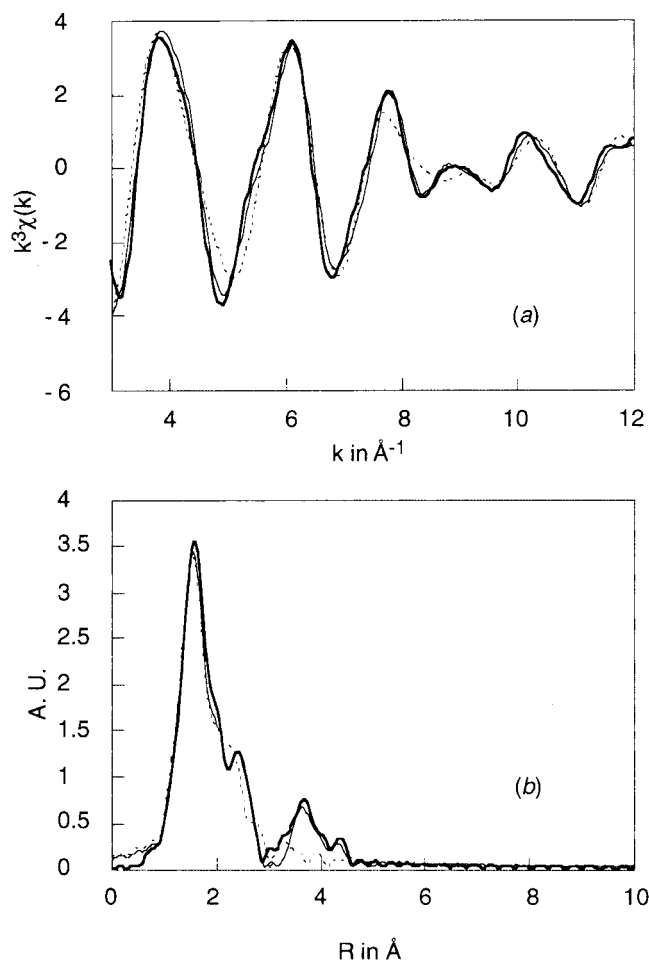


Figure 3. EXAFS data and simulations with CH₃CN for copper(II) complex 3: (a) $k^3\chi(k)$ and (b) radial distribution function (bold solid line, experimental signal; dashed line, simple scattering; straight solid line, multiple scattering).

of 2.0 Å and a Cu–S distance of 2.3 Å (values obtained after a single scattering analysis). Calculations with initial values for S_0^2 and $\langle\sigma^2\rangle$ give $R = 48\%$.

(ii) The scale factor and the global Debye–Waller factor for the multiple-scattering paths were optimized using a polynomial fitting. Final values are $S_0^2 = 1.1$, $\langle\sigma^2\rangle = 9.5 \times 10^{-3}$, and $R = 27\%$.

(iii) The atomic model was then minimized. The four atoms linked to the copper were expressed in spherical coordinates,

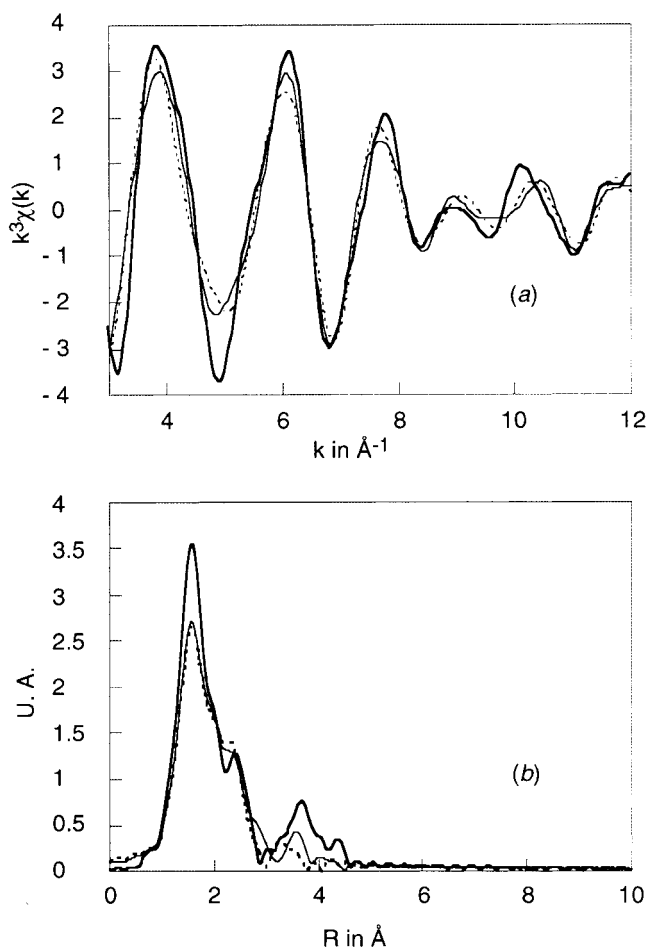


Figure 4. EXAFS data and simulations without CH₃CN for copper(II) complex 3: (a) $k^3\chi(k)$ and (b) radial distribution function (bold solid line, experimental signal; dashed line, simple scattering; straight solid line, multiple scattering).

and the minimization was performed by a simplex method with the X-Fine routine. At the end of this step, R is equal to 12%, Cu–S = 2.14 Å, Cu–N_t = 1.835 Å and Cu–N_{pyr} = 2.0 Å.

(iv) Constraints in the above model were relaxed by molecular modeling using prosimulate software.²⁵ Ten carbon atoms were included in the second shell, and the last refinement cycle was performed with individual Debye–Waller factors for each multiple-scattering path and converged with $R = 7.01\%$, on the two first shells (0.91–3 Å).

Final values of the EXAFS refinement as well as bond distances and σ^2 values found for complexes 2 and 3 are given in Table 3. The observed and the calculated EXAFS spectra and the radial distribution functions are given in Figures 3–6. Different situations are illustrated in order to point out the following two important features:

(i) Multiple scattering interactions can often contribute to the outer shell data, and these can arise either from the presence of rigid ligand groups such as imidazoles^{26,27} or in the case of a pathway involving an Fe–O–C unit.²⁸ This study offers the opportunity to draw attention to the effects of a linear ligand

(25) Oxford Molecular S. A., X-Pôle Ecole Polytechnique, F-91128 Palaiseau Cedex.

(26) Co, M. S.; Scott, R. A.; Hodgson, K. O. *J. Am. Chem. Soc.* **1981**, *103*, 986.

(27) Hasnain, S. S., Ed. *Synchrotron Radiation and Biophysics*; Ellis Horwood Ltd.: Chichester, U.K. 1990; Chapters 3 and 4.

(28) Westre, T. E.; Di Cicco, A.; Filippini, A.; Natoli, C. R.; Hedman, B.; Solomon, E. I.; Hodgson, K. O. *J. Am. Chem. Soc.* **1995**, *117*, 1566.

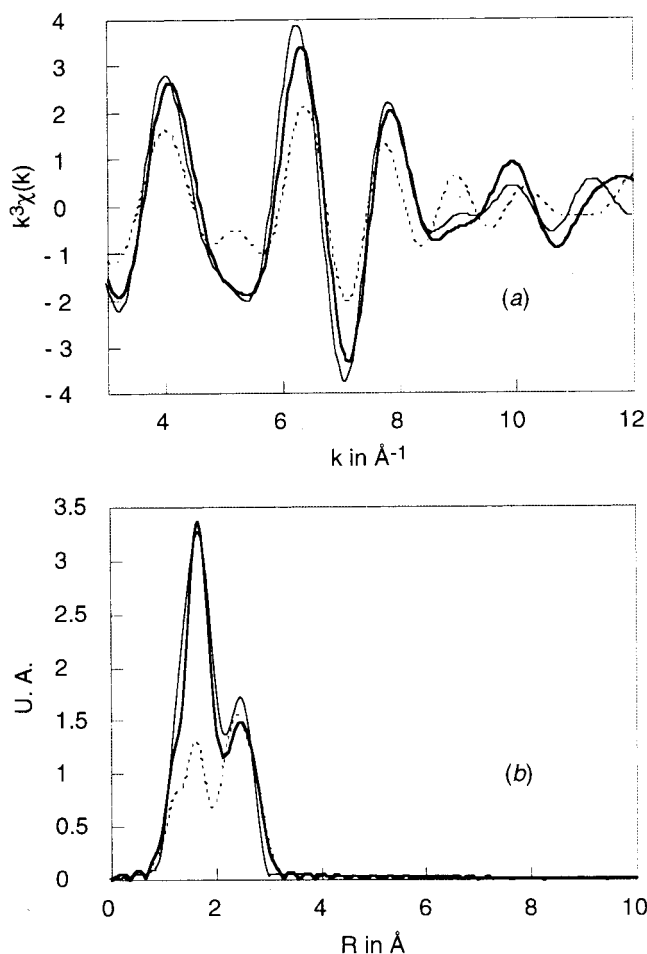


Figure 5. EXAFS data and simulations on first and second shells for copper(II) complex **3**: (a) $k^3\chi(k)$ and (b) radial distribution function (bold solid line, experimental signal; dashed line, simulation without S; straight solid line, simulation with S).

like CH₃CN (Figures 3 and 4). When multiple scattering is neglected, the experimental curve can be fitted; however the corresponding Cu–S distance is not acceptable, 2.40 Å vs 2.335(1) Å for the crystallographic value. A shift of the S-peak is also observed when the CH₃CN contribution is not taken into account in the FEFF calculations, and the experimental curve cannot be fitted, even giving Cu–S the crystallographic value. Therefore, it can be said that CH₃CN is the major source of the multiple scattering effects on the first and second shells in compound **3**.

(ii) The presence of the S atom in the copper coordination sphere of compound **2** is clearly demonstrated in Figure 6.²⁹ For this compound, the second peak of the radial distribution curve is not adequately modeled, and it is likely that there are multiple-scattering contributions from the aromatic groups. However, in the absence of CH₃CN, the multiple scattering is less important, and the results are reliable.

Structures of complexes **2** and **3** are marked by some features which have been identified by this combined crystallographic

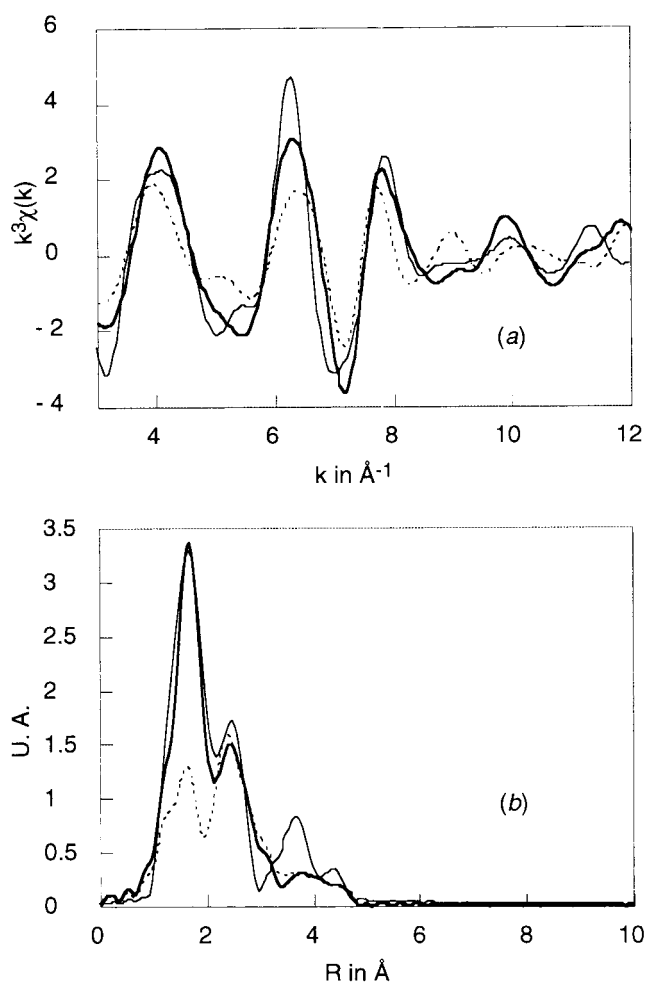


Figure 6. EXAFS data and simulations on whole signal for copper(I) complex **2**: (a) $k^3\chi(k)$ and (b) radial distribution function (bold solid line, experimental signal; dashed line, simulation without S; straight solid line, simulation with S).

and XAS study. The change in the coordination geometry from a square-plane pyramid to a distorted tetrahedron is also completed by a shortening of the copper(I)-to-ligand distances. The most important variations are observed for the Cu–S distance, 2.34 Å in **3** and 2.14 Å in **2**, and for the Cu–N distance, 2.06 Å in **3** and 1.84 Å in **2**. According to the Cambridge Data Bank, such a short Cu(I)–N distance has been found in more than 20 crystallographic structures in which the nitrogen atoms have an sp₂ (enamine or aromatic) and an sp₃ (five- or six-membered metallo-ring) hybridization (Scheme 3).

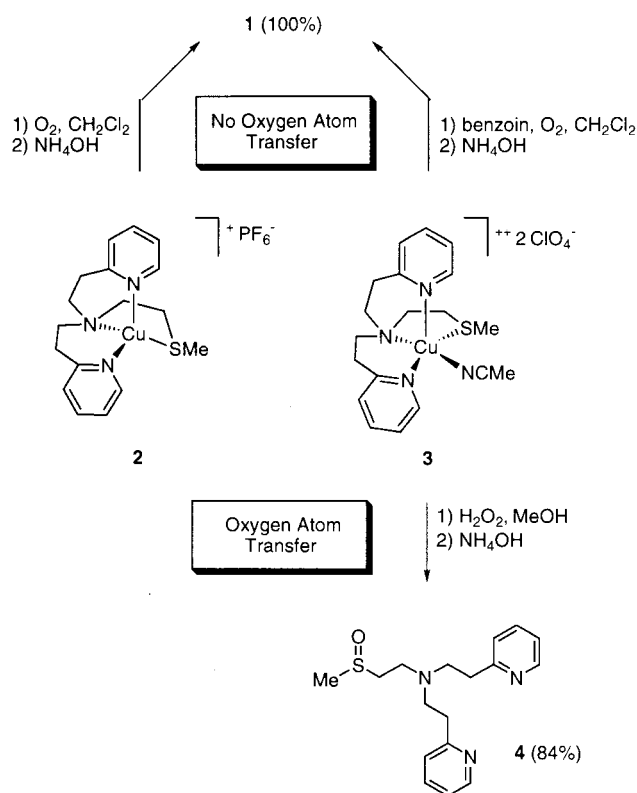
Reactivity with O₂ and H₂O₂. We did not detect any ligand oxidation with complexes derived from MeSPY2, **1**, ligand, contrary to those complexes [RPY2]CuPF₆ for which oxygen atom transfers to the ligand (OATL) were observed upon dioxygen exposure.^{30,31} The clear yellow CH₂Cl₂ solution (1 mM) of [MeSPY2]CuPF₆, **2**, complex rapidly turned into a green solution upon exposure to an O₂ atmosphere. The stoichiometry of Cu/O₂ measured by manometry was 4:1. Precipitation with diethyl ether afforded a green powder corresponding to a copper(II) complex which released, in quantitative yield, unchanged ligand **1** after demetalation with a 35% NH₄OH solution. The same result was obtained by reaction of the

(29) The presence of the MeS group in the copper coordination sphere of compound **2** is confirmed both by ¹H and ¹³C NMR spectra where large downfield effects are observed on MeS resonances ($\Delta\delta_2 - \Delta\delta_1 = 2.21 - 2.03 = 0.18$ ppm for ¹H and $\Delta\delta_2 - \Delta\delta_1 = 18.77 - 15.60 = 3.20$ ppm for ¹³C). See: Karlin, K. D.; Haka, M. S.; Cruse, R. W.; Meyer, G. J.; Farooq, A.; Gultneh, Y.; Hayes, M. S.; Zubieta, J. J. *Am. Chem. Soc.* **1988**, *110*, 1196. Gagne, R. R.; Kreh, R. P.; Dodge, J. A.; Marsh, R. E.; McCool, M. *Inorg. Chem.* **1982**, *21*, 254. Nelson, S. M.; Lavery, A. Drew, M. G. B. *J. Chem. Soc., Dalton Trans.* **1986**, 911.

(30) Amadéi, E.; Alilou, E. H.; Eydoux, F.; Pierrot, M.; Réglie, M.; Waegell, B. *J. Chem. Soc., Chem. Commun.* **1992**, 1782.

(31) Itho, S.; Kondo, T.; Komatsu, M.; Ohshiro, Y.; Li, C.; Kanehisa, N.; Kai, Y.; Fukuzumi, S. *J. Am. Chem. Soc.* **1995**, *117*, 4714.

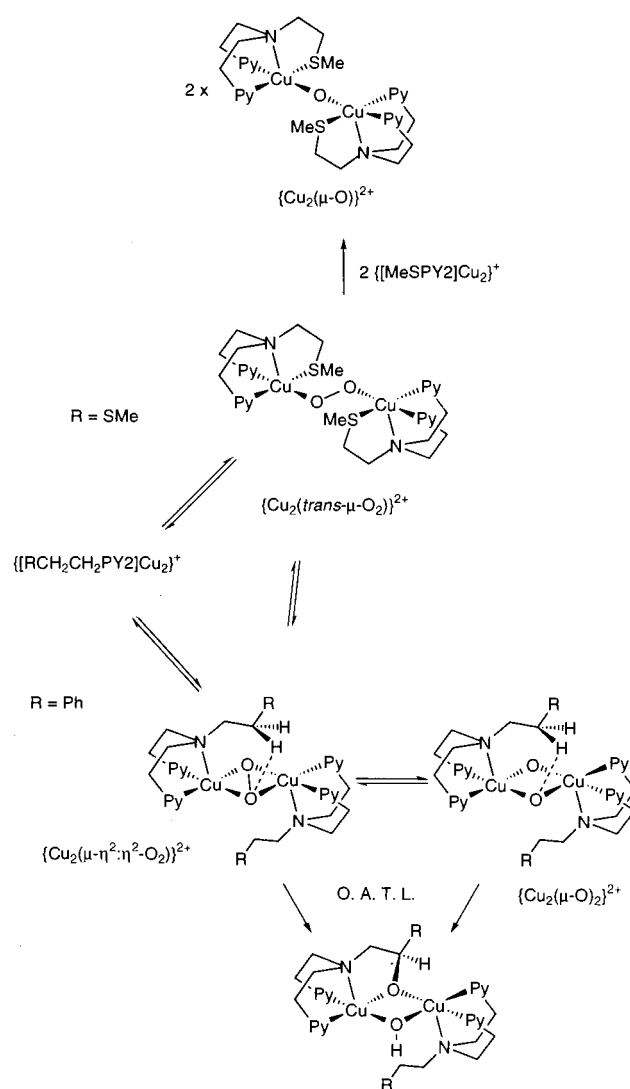
Scheme 3



copper(II) complex $[\text{MeSPY2}]\text{Cu}(\text{ClO}_4)_2$, **3**, with dioxygen in the presence of reductant (benzoin/ NEt_3 ²⁹ or ascorbate/phosphate buffer pH 7.4).³²

Copper/dioxygen chemistry is well documented.³³ The structures of copper(II) peroxy species formed upon dioxygen exposure depend on the ligand. Indeed, with tridentate ligands (RPY2,³⁴ $\text{HB}(3,5\text{-iPr}_2\text{pz})_3$,³⁵ and iPr_3tacn ³⁶), copper(I) species are known to lead to side-on ($\mu\text{-}\eta^2\text{:}\eta^2\text{-peroxy}$)dicopper(II) species upon reaction with O_2 . It was shown that side-on peroxy species which possess nonbasic/electrophilic properties³⁷ have oxidizing capability toward cyclohexene³⁸ and PPh_3 .³⁹ In some cases, this side-on peroxy species have the capability to insert an oxygen atom into a C–H bond of the ligand.⁴⁰ Recently, Tolman et al. have reported that ($\mu\text{-}\eta^2\text{:}\eta^2\text{-peroxy}$)dicopper(II) species can exist in equilibrium with a bis($\mu\text{-oxo}$)dicopper(III) species.⁴¹ These authors proposed that $\{\text{Cu}_2(\mu\text{-}\eta^2\text{:}\eta^2\text{-O}_2)\}^{2+}$ and $\{\text{Cu}_2(\mu\text{-O})_2\}^{2+}$ cores are isomers residing at the same

Scheme 4

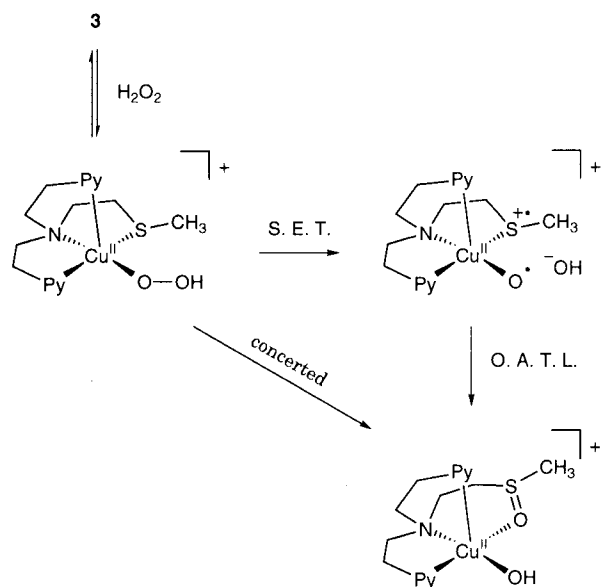


overall oxidation level and, therefore, each can be considered equally competent as potential oxidants in copper/dioxygen chemistry. Such $\{\text{Cu}_2(\mu\text{-}\eta^2\text{:}\eta^2\text{-O}_2)\}^{2+}$ and $\{\text{Cu}_2(\mu\text{-O})_2\}^{2+}$ intermediates could be responsible for observed OATL in $[\text{RPY2}]\text{CuPF}_6$ chemistry (Scheme 4).^{30,31} Tripodal tetradentate ligand such as TMAPA⁴² and quinoyl-substituted⁴³ and binucleating analogues⁴⁴ give copper(I) complexes which bind O_2 to

- (32) Uchida, K.; Kawakishi, S. *Biochim. Biophys. Acta* **1990**, *347*, 1034.
 Uchida, K.; Kawakishi, S. *Arch. Biochem. Biophys.* **1990**, *283*, 20.
 (33) Karlin, K. D.; Kaderli, S.; Zuberbühler, A. D. *Acc. Chem. Res.* **1997**, *30*, 139.
 (34) Sanyal, I.; Mahroof-Tahir, M.; Nasir, S.; Ghosh, P.; Cohen, B. I.; Gultneh, Y.; Cruse, R.; Farooq, A.; Karlin, K. D.; Liu, S.; Zubieta, J. *Inorg. Chem.* **1992**, *31*, 4322. Blackburn, N. J.; Strange, R. W.; Farooq, A.; Haka, M. S.; Karlin, K. D. *J. Am. Chem. Soc.* **1988**, *110*, 4263.
 (35) Kitajima, N.; Fujisawa, K.; Moro-Oka, Y. *J. Am. Chem. Soc.* **1989**, *111*, 8975. Kitajima, N.; Moro-Oka, Y. *Chem. Rev.* **1994**, *94*, 737.
 (36) Mahapatra, S.; Halfen, J. A.; Wilkinson, E. C.; Que Jr., L.; Tolman, W. B. *J. Am. Chem. Soc.* **1994**, *116*, 9785.
 (37) Paul, P. P.; Tyeklar, Z.; Jacobson, R. R.; Karlin, K. D. *J. Am. Chem. Soc.* **1991**, *113*, 5322.
 (38) Kitajima, N.; Koda, T.; Iwata, Y.; Moro-Oka, Y. *J. Am. Chem. Soc.* **1990**, *112*, 8823.
 (39) Karlin et al. have observed PPh_3 oxidation with spectroscopically characterized side-on ($\mu\text{-}\eta^2\text{:}\eta^2\text{-peroxy}$)dicopper(II) species derived from RPY2 ligands.³⁵ However, with X-ray characterized ($\mu\text{-}\eta^2\text{:}\eta^2\text{-peroxy}$)dicopper(II) species derived from $\text{HB}(3, 5\text{-iPr}_2\text{pz})_3$ ligand, Kitajima et al. observed the formation of $\text{Cu}(\text{I})\text{-PPh}_3$ complexes with concomitant liberation of O_2 and no PPh_3 oxidation.³⁶

- (40) Karlin, K. D.; Hayes, J. C.; Gultneh, Y.; Cruse, R. W.; McKown, J. W.; Hutchinson, J. P.; Zubieta, J. *J. Am. Chem. Soc.* **1984**, *106*, 2121. Mahapatra, S.; Halfen, J. A.; Wilkinson, E. C.; Que, L., Jr.; Tolman, W. B. *J. Am. Chem. Soc.* **1994**, *116*, 9785. Mahapatra, S.; Halfen, J. A.; Wilkinson, E. C.; Pan, G.; Cramer, C. J.; Que, L., Jr.; Tolman, W. B. *J. Am. Chem. Soc.* **1995**, *117*, 8865. Halfen, J. A.; Young, V. G., Jr.; Tolman, W. B. *J. Am. Chem. Soc.* **1996**, *118*, 10920. Allen, W. E.; Sorrell, T. N. *Inorg. Chem.* **1997**, *36*, 1732.
 (41) Halfen, J. A.; Mahapatra, S.; Wilkinson, E. C.; Kaderli, S.; Young, V. C., Jr.; Que, L., Jr.; Zuberbühler, A. D.; Tolman, W. B. *Science* **1996**, *271*, 1397. Mahapatra, S.; Halfen, J. A.; Wilkinson, E. C.; Pan, G.; Xuedong, W.; Young, V. C., Jr.; Cramer, C. J.; Que, L., Jr.; Tolman, W. B. *J. Am. Chem. Soc.* **1996**, *118*, 11555. Mahapatra, S.; Halfen, J. A.; Tolman, W. B. *J. Am. Chem. Soc.* **1996**, *118*, 11575.
 (42) Jacobson, R. R.; Tyeklar, Z.; Farooq, A.; Karlin, K. D.; Liu, S.; Zubieta, J. *J. Am. Chem. Soc.* **1988**, *110*, 3690. Tyeklar, Z.; Jacobson, R. R.; Wei, N.; Murthy, N. N.; Zubieta, J.; Karlin, K. D. *J. Am. Chem. Soc.* **1993**, *115*, 2677.
 (43) Karlin, K. D.; Wei, N.; Jung, B.; Kaderli, S.; Niklaus, P.; Zuberbühler, A. D. *J. Am. Chem. Soc.* **1993**, *115*, 9506.
 (44) Lee, D.-H.; Wei, N.; Murthy, N. N.; Tyeklar, Z.; Karlin, K. D.; Kaderli, S.; Jung, B.; Zuberbühler, A. D. *J. Am. Chem. Soc.* **1995**, *117*, 12498.

Scheme 5

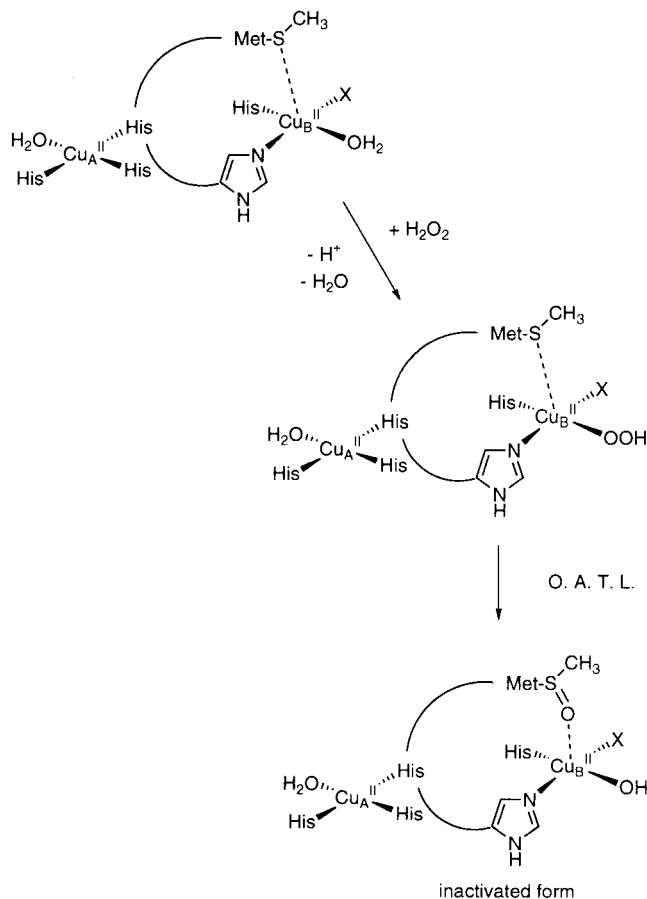


give end-on *trans*-(μ -1,2-peroxy)dicopper(II) products. Contrary to the side-on species, the end-on peroxide moieties are basic/nucleophilic³⁵ and react with PPh₃ to give Cu(I)-PPh₃ complexes with concomitant liberation of O₂, and no ligand oxidations are observed. Although it was not possible to detect any peroxy species by UV-vis spectroscopy (even at low temperature in CH₂Cl₂, -80 °C), MeSPY2, **1**, is a tetradentate ligand, and it is reasonable to propose the formation of a *trans*-(μ -1,2-peroxy) species upon reaction of [MeSPY2]CuPF₆, **2**, with O₂. This intermediate which is basic/nucleophilic reacts with the electrophilic copper(I) complex **2** with O-O bond cleavage leading to a μ -oxo-Cu(II) complex (O₂ 4 e⁻ reduction).

More interesting is the reaction of the copper(II) complex [MeSPY2]Cu(ClO₄)₂, **3**, with hydrogen peroxide. In the presence of an excess of H₂O₂ (10 equiv in MeOH at room temperature) copper(II) complex **3**, after demetalation (35% NH₄OH solution), gave 84% of a new compound **4**. A thorough analysis of the spectral data compared with those of an authentic sample obtained by oxidation of ligand **1** with *meta*-chloroperbenzoic acid indicated that the sulfoxide **4** is the oxidation product of the ligand sulfide group.

As mentioned in the Introduction, the mechanism of DBH catalysis has been a subject of many studies^{6,7} from which it is well established that a Cu(II)-OOH species formed by oxygen activation is responsible for the hydroxylation of dopamine. May et al. have reported that DBH catalyzes the conversion of phenyl-2-aminoethyl sulfides to the corresponding sulfoxides at a rate which is considerably higher than the hydroxylation of the corresponding carbon analogues.⁴⁵ On the other hand, recent studies of Karlin's group on copper-dioxygen chemistry have shown that Cu(II)-OOH species are able to transfer an oxygen atom to tetrahydrothiophene, giving the corresponding sulfoxide.⁴⁶ Therefore, taking into account these results, we can reasonably propose that the first step of the reaction is the formation of a [MeSPY2]Cu(II)-OOH species. Then, the

Scheme 6. Mechanisms Proposed for Hydrogen Peroxide Inactivation of DBH and PHM



oxygen atom transfer to the sulfide group could occur by a concerted mechanism; however, a single-electron transfer of the sulfide group leading to MeS⁺ and Cu(II)-O[•] radical species may be also considered. The strong tendency of the MeS⁺ toward sulfoxidation produces the sulfoxide by rebounding with Cu(II)-O[•] radical species (Scheme 5).

Conclusion and Biological Relevance

The Cu_B(His)₂X(H₂O) four-coordinated geometry (without strong SMe binding) known for DBH and PHM is quite distinct from the square pyramidal CuN₄S geometry (with strong equatorial SMe binding) of the copper complex **3** described in this paper. Our work has the merit to clarify some observations reported for the inactivation of DBH and PHM by hydrogen peroxide, and thus **3** can be considered as a good functional model.⁴⁷ Indeed, some years ago Skotland and Ljones reported irreversible inactivation of the water soluble form of bovine adrenal DBH by hydrogen peroxide (or ascorbate) in the absence of any substrate.⁴⁸ More recently, the same irreversible inactivation was reported by Merkler et al. for PHM.⁴⁹ Considering that the H₂O₂ (or ascorbate)-inactivated DBH binds copper more weakly than the native form, it was proposed that

(45) May, S. W.; Phillips, R. S. *J. Am. Chem. Soc.* **1980**, *102*, 5981.
 (46) Karlin, K. D.; Ghosh, P.; Cruse, R. W.; Farooq, A.; Gultneh, Y.; Jacobson, R. R.; Blackburn, N. J.; Strange, R. W.; Zubieta, J. *J. Am. Chem. Soc.* **1988**, *110*, 6769. Mahroof-Tahir, M.; Murthy, N. N.; Karlin, K. D.; Blackburn, N. J.; Shaikh, S. N.; Zubieta, J. *Inorg. Chem.* **1992**, *31*, 3001. Karlin, K. D.; Cruse, R. W.; Gultneh, Y. *J. Chem. Soc., Chem. Commun.* **1987**, 599.

(47) Further modeling is needed to design the best copper ligand to achieve hydroxylation as in DBH and PHM. The approach used here needs to be improved to attain the goal of a copper complex with catalytic hydroxylation properties toward exogenous ligands. Thus, the problem to achieve association of the substrate into the copper coordination sphere still remains to be solved.
 (48) Skotland, T.; Ljones, T. *Arch. Biochem. Biophys.* **1979**, *201*, 81.
 (49) Merkler, D. J.; Kulathila, R.; Tamburini, P. P.; Young, S. D. *Arch. Biochem. Biophys.* **1992**, *294*, 594.

the enzyme-bound copper catalyzes the partial destruction of its own binding site by hydroxylation of one histidine residue. This hypothesis was supported by Uchida and Kawakishi who observed histidine-residue hydroxylation of angiotensin by copper(II) salts in the presence of ascorbate and dioxygen.³² However, in the light of the recent XAS studies of DBH and PHM active sites which show the presence of Met³¹⁴ and taking into account our present findings, we suggest that Met³¹⁴ could be the site of the inactivation by oxidation into a sulfoxide group (Scheme 6). Confirmation of these proposals and characterization of the modified protein will certainly provide valuable

information about the active site of DBH whose crystal structure is still lacking. This work is in progress in our group.

Acknowledgment. We acknowledge the use of the synchrotron radiation facilities and the help given by personnel at LURE and, more particularly, Dr. Isabella Ascone.

Supporting Information Available: Tables of positional and thermal parameters, interatomic distances and angles, and general displacement parameter expressions (*B*'s) for compound **3** (10 pages). Ordering information is given on any current masthead page.

IC9709281